To be presented at the 6th International Conference on
Advances in Materials Technology for Fossil Power Plants
La Fonda, Santa Fe, New Mexico, USA, August 31st – September 3rd, 2010

The effect of simulated post weld heat treatment temperature overshoot on microstructural evolution in P91 and P92 power plant steels

R.C. MacLachlan[1], J.J. Sanchez-Hanton[2] and R.C. Thomson[1]

[1]Department of Materials, Loughborough University, Loughborough, LE11 3TU, UK
[2]RWE npower, Electron, Windmill Hill Business Park, Whitehill Way, Swindon, Wiltshire, SN5 6PB, UK

ABSTRACT

Creep strength enhanced ferritic (CSEF) steels, in particular modified 9Cr steels Grade 91 and 92, are becoming more widely used in the electrical power generation industry for the construction of header and steam piping in advanced coal-fired power plants. They typically enter service having received a standard high temperature normalizing treatment following by a lower temperature tempering treatment designed to produce an optimum microstructural condition. However, situations may arise in practice, particularly during welding operations for example, whereby the component may receive an additional heat treatment which briefly exceeds the Ac_1, and possibly the Ac_3, temperature before stabilizing at the tempering temperature.

In this research, simulated post weld heat treatments (PWHT) have been applied to Grade 91 and 92 materials using carefully controlled heating and cooling rates within a dilatometer. Peak temperatures applied were below Ac_1, between Ac_1 and Ac_3, and above Ac_3, prior to a subsequent heat treatment at 750^{o}C for 2 hours. Hardness measurements demonstrated a significant reduction once the Ac_1 temperature was exceeded.

Advanced electron microscopy has been carried out to investigate the effect of the PWHT excursions on subsequent microstructural evolution. Electron back scatter diffraction has been used to quantify the nature of the martensite laths and grain structure changes as a function of temperature. The detailed size distribution of carbides within the microstructure has also been determined using both scanning and transmission electron microscopy. These results are discussed in respect of the likely consequences of such a PWHT overshoot on subsequent mechanical properties during high temperature service.

1. Introduction

Creep strength enhanced ferritic (CSEF) steels, in particular modified 9Cr steels Grade 91 and 92, are becoming more widely used in the electrical power generation industry for the construction of header and steam piping in advanced coal-fired power plants. This is due to a combination of highly desirable properties, such as excellent elevated temperature strength and creep resistance[1-3]. The microstructure consists of a tempered martensite matrix, a fine dispersion of intergranular chromium-rich $M_{23}C_6$ precipitates, as well as intragranular carbonitride MX precipitates rich in V and Nb. This microstructure is produced following a normalizing and tempering heat treatment at temperatures in the region of 1050°C and 750-770°C respectively.

The microstructure of the as-manufactured material, which is designed for specific service conditions, may be altered by the application of additional heat treatment and welding procedures to the material in power plant. Welding processes conventionally involve a post weld heat treatment (PWHT) to relieve residual stresses. Situations may arise whereby pipe which has received a correct normalising and tempering treatment prior to welding, is subject to an accidental 'overshoot' in temperature during PWHT. The temperature may rise, albeit briefly, above 800°C and therefore above the Ac_1 temperature of the steel before stabilising at the stress relief temperature of ~765°C. It is extremely important to understand the effects of undesired PWHT temperature excursions on the pre-service parent microstructure, and its evolution during service, on the creep behaviour of high temperature steam pipework.

2. Experimental Methods

2.1 Materials and Heat Treatments

The materials used in this research were two 9 wt.% Cr steels designated Grades 91 and 92, in the form of pipe sections, hence subsequently designated as P91 and P92. Their chemical compositions are shown in Table 1. The materials had received typical commercial normalizing and tempering treatments, but had not seen any subsequent heat treatments or service. Samples were machined into cylinders of 5 mm diameter and 10 mm long for heat treatment in a dilatometer. Additional larger samples were available for heat treatment in a furnace to obtain similar microstructures to those which were obtained from the dilatometer heat treatments. These samples were creep test blanks, of dimensions 150 mm x 20 mm x 20 mm and following heat treatment, they were subsequently machined into standard creep samples consistent with BS EN 10219:2000.

Table 1: Chemical compositions of the steels used, balance Fe /wt.%

	C	Si	Mn	S	Cr	Mo	Ni	Al	Ti	Nb	V	N	W
P91	0.10	0.27	0.43	0.002	8.70	1.08	0.32	0.01	0.005	0.07	0.24	0.073	0.02
P92	0.10	0.26	0.40	0.001	9.13	0.44	0.23	0.01	0.001	0.06	0.20	0.045	1.83

A number of different heat treatments were carried out in a Baehr-Thermoanalyse DIL 805 dilatometer, which was able to control the heat treatments accurately, monitor the change in length as a result of phase transformation, and was operated in a vacuum to prevent decarburisation and oxidation occurring. Cooling was carried out using helium gas, which was able to achieve rates of up to 90°C s^{-1}.

In order to determine the Ac_1 and Ac_3 temperatures for the steels, the samples were initially rapidly heated to 600°C, and were then heated further to 1100°C at a rate of 8.3°C min^{-1}. The samples were subsequently quenched to room temperature at a rate of 90°C s^{-1}. These conditions were chosen after a number of experimental trials which demonstrated that there was very little variation in the Ac_1 and Ac_3 temperatures obtained with heating rates less than 20°C min^{-1}.

The main purpose of this investigation was to examine the effect of a possible overshoot above the normal tempering temperature (~750^{o}C) for these steels, for example, during a post weld heat treatment. Therefore, a series of simulated tempering treatments were carried out in which samples were heated at a rate of 50^{o}C min^{-1} to peak temperatures which varied between 800 and 960^{o}C in 20^{o}C steps, held at the peak temperature for 60 s, then subsequently cooled to 750^{o}C at a rate of 5^{o}C min^{-1} where they were held for 2 h before final cooling at a rate of 90^{o}C s^{-1} to room temperature.

2.2 Thermodynamic Calculations

Thermodynamic calculations were carried out to give an indication of the phases likely to be present at equilibrium in the steels using the software package MTDATA[4] in conjunction with the critically assessed thermodynamic database for ferrous materials, TCFE[5] version 1.22. Calculations were carried out over the temperature range 500 to 1500^{o}C, and the phases liquid, ferrite, austenite, various carbides, Laves, sigma and AlN were allowed to exist in the calculations.

2.3 Optical Microscopy and Hardness Measurements

Samples were sectioned after heat treatment using a Struers Accutom saw, using an alumina slitting disk. The samples were subsequently mounted in conducting Bakelite, followed by grinding using 240 to 1200 grit SiC in a resin bond, and polishing on standard cloths with diamond suspensions down to 1 μm. Samples for examination using electron back scatter diffraction were further polished with a 0.02 μm colloidal silica suspension. Etching was carried out for optical microscopy using Villela's reagent (1 g picric acid, 5 ml hydrochloric acid and 100 ml ethanol) for approximately 30 s. The samples were imaged using an inverted Reichert-Jung MeF3 optical microscope, with the images captured digitally using a Fujitsu HC-300Z digital camera. Macrohardness testing was carried out using a Mitutoyo AVK-C2 hardness tester with a load of 10 kg and a dwell time of 15 s. Microhardness testing was also carried out within specific phases present within the microstructure using a Mitutoyo-HM instrument. A diamond indenter was used with a dwell time of 15 s and a load of 5 g to ensure that the indent was only in the phase of interest.

2.4 Scanning Electron and Focussed Ion Beam Microscopy

Scanning electron microscopy was carried out primarily in a Zeiss 1530VP field emission gun system (FEGSEM) using an accelerating voltage of 20 kV, an aperture of 20 μm and a working distance of 9 mm for imaging. An fei Nova Nanolab 600 dual beam field emission gun scanning electron microscope and ion beam system (FIBSEM) was also used for both characterizing the grain structure and the carbide population using ion beam etching[6], and also for the preparation of site specific samples for transmission electron microscopy (TEM). The gallium ion beam was rastered across the sample surface at a speed of 150 μm s^{-1} to produce a contrast gradient between the second phase particles and the matrix using an accelerating voltage of 30 kV, current of 50 pA, an aperture of 10 μm at a working distance of 16 mm. Both microscopes were equipped with an EDAX Pegasus combined electron back scatter diffraction (EBSD) and energy dispersive X-ray analysis (EDX) analytical system. EBSD was used for quantification of the grain size and orientation using an EDAX Hikari camera with a mean step size of 0.1 μm, a working distance of 16 mm and an aperture of 60 μm. Image analysis using the ImageTool software package was used using a minimum of 5 images per sample. The resolution limit using this technique was ~25 nm.

2.5 Transmission Electron Microscopy

Transmission electron microscopy (TEM) was carried out in a Jeol 2000FX microscope operating at 200 kV. Images were captured using an Erlanshen ES500W digital camera. Two types of sample were examined: carbon extraction replicas were used to obtain chemical composition information from the carbide particles without interference from the ferrous matrix, and site specific thin foil samples prepared using the FIBSEM were used to determine the nature of particular phases present within the matrix. The TEM was equipped with an Oxford Instruments Inca EDX system.

3. Results and Discussion

3.1 Thermodynamic Calculations

The main phases predicted to be present at thermodynamic equilibrium in both the P91 and P92 steels were the ferritic matrix, together with ~2 % by weight of $M_{23}C_6$ (Cr rich) and ~0.5 % by weight of MX (both V and Nb rich). In addition, in the P92 steel which has a significant addition of W, the Laves phase was predicted to be present below 700°C, rising to ~ 2.5 % by weight at 500°C. The key phase transformation temperatures calculated are presented in Table 2. The values predicted for Ae_1 are within the range quoted for Ac_1 of ~800-830°C, whereas values for Ae_3 are predicted to be lower than the quoted values for Ac_3 of 890-940°C for P91 and 900-920°C for P92 respectively[1,2]. These differences are attributable to the differences between equilibrium calculations and phase transformation temperatures measured on heating a sample.

Table 2: Phase transformation temperatures determined using thermodynamic calculations / Temperatures in °C

Material	Ae_1	Ae_3	50% $M_{23}C_6$ dissolution	$M_{23}C_6$ dissolution	Delta ferrite formation on heating	Liquid formation on heating
P91	800	847	840	868	1292	1441
P92	818	889	857	891	1191	1430

In P91 and P92 respectively, the dominant $M_{23}C_6$ carbides were predicted to completely dissolve at 868°C and 891°C, however, it is interesting to note that delta ferrite was predicted to form at a temperature approximately 100°C lower in the P92 material than in the P91, presumably due to the presence of W which is a strong ferrite stabilizing element.

3.2 Characterisation of the As-received Microstructure

The as-received microstructures for both the P91 and P92 steels were observed to be primarily martensitic using optical metallography, with hardnesses of 200 Hv_{10} and 205 Hv_{10} respectively. It was, however, observed that there were small 'island' regions of ~10 μm in extent, which appeared to contain no sub-structure, within the P92 material. It was demonstrated that a subsequent normalization heat treatment at 1050°C followed by quenching to room temperature was able to remove these 'islands'. Microhardness indicated that these regions were slightly harder (by ~15 Hv_{10}) than the remainder of the matrix. Site-specific TEM sample preparation followed by selected area electron diffraction was able to confirm that these regions were in fact ferritic, with a high dislocation density observed which is consistent with the microhardness value obtained, and also a higher concentration of both Cr and W (ferrite stabilizers) than the surrounding matrix. It is postulated that the ferrite is present during the initial high temperature heat treatment of the steel, perhaps during a rolling operation which might be carried out at a temperature higher than the delta ferrite formation temperature, and that this structure can be retained to lower temperatures depending on the process heat treatments carried out.

The Ac_1 and Ac_3 temperatures were determined for both materials using dilatometry using the heat treatment parameters described above. It was also possible to determine the start temperature of the martensite transformation, M_S, for both materials during subsequent quenching to room temperature. The phase transformation temperatures determined by dilatometry, and the hardness of the resulting as quenched microstructures, are presented in Table 3. These temperatures are consistent with values quoted[1,2] in the literature; an M_s of ~400°C has been observed for both P91 and P92.

Table 3: Phase transformation temperatures determined using dilatometry

Material	Ac_1 /°C	Ac_3 /°C	M_S /°C	Hardness /Hv_{10}
P91	813±3	921±6	388±8	439
P92	854±4	929±7	412±6	426

3.3 Simulated Post Weld Heat Treatments

A series of simulated post weld heat treatments (PWHT) were carried out in a dilatometer as described in section 2.1 with peak temperatures between 800°C, below the Ac_1 temperature, and 960°C, which is above the Ac_3 temperature. Examples of the change in length data obtained from dilatometry are presented in Figure 1 for P91 (a) and P92 (b) respectively for peak temperatures of 800°C and 900°C. It can be seen that there is a clear difference between the curves for each of the two temperatures, with the curve for 900°C showing that a phase transformation to austenite begins during the heating cycle.

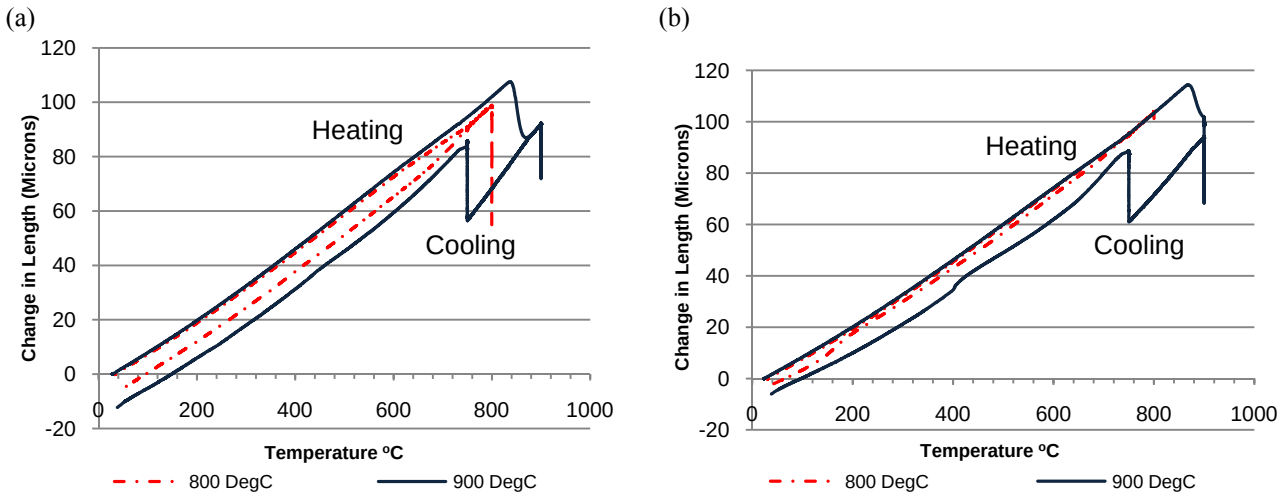

Figure 1: Dilatometry data showing the change in length of (a) P91 and (b) P92 as a function of temperature for both heating and cooling, when subjected to a post weld heat treatment 'overshoot' at temperatures of 800°C and 900°C.

The hardness data following a simulated PWHT overshoot at temperatures between 800°C and 960°C are presented in Figure 2 for P91 (a) and P92 (b) respectively. In general, similar hardness decreases are observed for both materials, although the P92 material has a hardness of ~10 Hv_{10} lower than P91 at the highest overshoot temperatures. It can be seen that for P91 the hardness begins to drop significantly at 840°C, whereas in the P92 a temperature of 860°C is required before there is a significant drop in the hardness. The predicted $M_{23}C_6$ dissolution is also plotted on the same axes from the thermodynamic calculations. It is noted that $M_{23}C_6$ is predicted to remain stable to slightly higher temperatures in the P92 material, which is consistent with the hardness drop commencing at a higher overshoot temperature in P92 compared to P91.

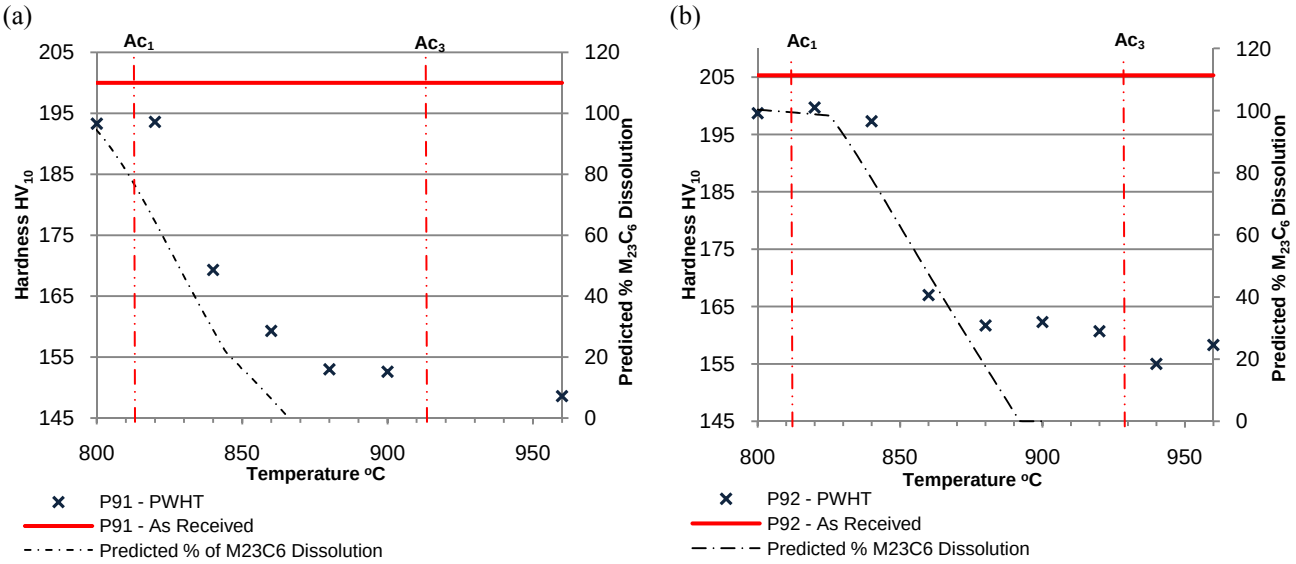

Figure 2: Hardness data for P91 (a) and P92 (b) after PWHT overshoots at temperatures between 800°C and 960°C. The measured values of Ac_1 and Ac_3 are also shown, together with the predicted amount of $M_{23}C_6$ dissolution from the thermodynamic calculations as a function of temperature.

Optical micrographs after PWHT overshoot heat treatments at 800°C, 860°C and 900°C for both P91 and P92 are presented in Figure 3. After the 800°C heat treatment, the microstructure appears fully martensitic, with a well-defined lath structure. Comparison with the micrographs for the 900°C heat treatment shows that the structure has begun to 'disintegrate' and the martensite laths are much less clearly defined. A gradual coarsening of the microstructure is also observed with increasing peak heat treatment temperature and there are indications that the microstructure is no longer single phase martensite but instead comprises additional matrix phases. Examples of the 'islands' visible in the P92 material can be seen in Figure 3d.

The optical microstructures show some evidence of mixed microstructures, and the dilatometry data provide evidence of the reverse transformation to austenite occurring on heating and subsequent transformation to ferrite on holding at 750°C. Therefore, in order to further investigate the nature of the matrix microstructure as a function of peak heat treatment temperature, EBSD was carried out on all samples as described in section 2.4. EBSD images from representative P92 samples are presented, however, similar results were also obtained for the P91 material. Figure 4 illustrates the image quality maps derived from the EBSD scans which present a high resolution image of the grain/lath structure. Figure 5 presents the corresponding grain boundary maps in which high angle boundaries have been defined to be greater than 15° (coloured in blue), and low angle boundaries are in the range 2-5° (coloured in red), and boundaries between 5 and 15° coloured in green. The martensitic nature is clearly visible in Figures 4a and 5a after a PWHT overshoot at 800°C, and there is evidence of some coarsening in Figures 4b and 5b after a PWHT overshoot at 880°C. Once a peak temperature of 900°C is reached, little evidence of the martensitic lath structure remains (Figures 4c and 5c), broadly consistent with the changes observed using optical microscopy. Figures 4d and 5d show that after a PWHT overshoot at 960°C followed by a standard temper at 750°C for 2 hours, there are relatively large grains present in the microstructure, of size ~10-20 μm, which is dominated by high angle grain boundaries much reduced in length compared to those at the lower temperatures.

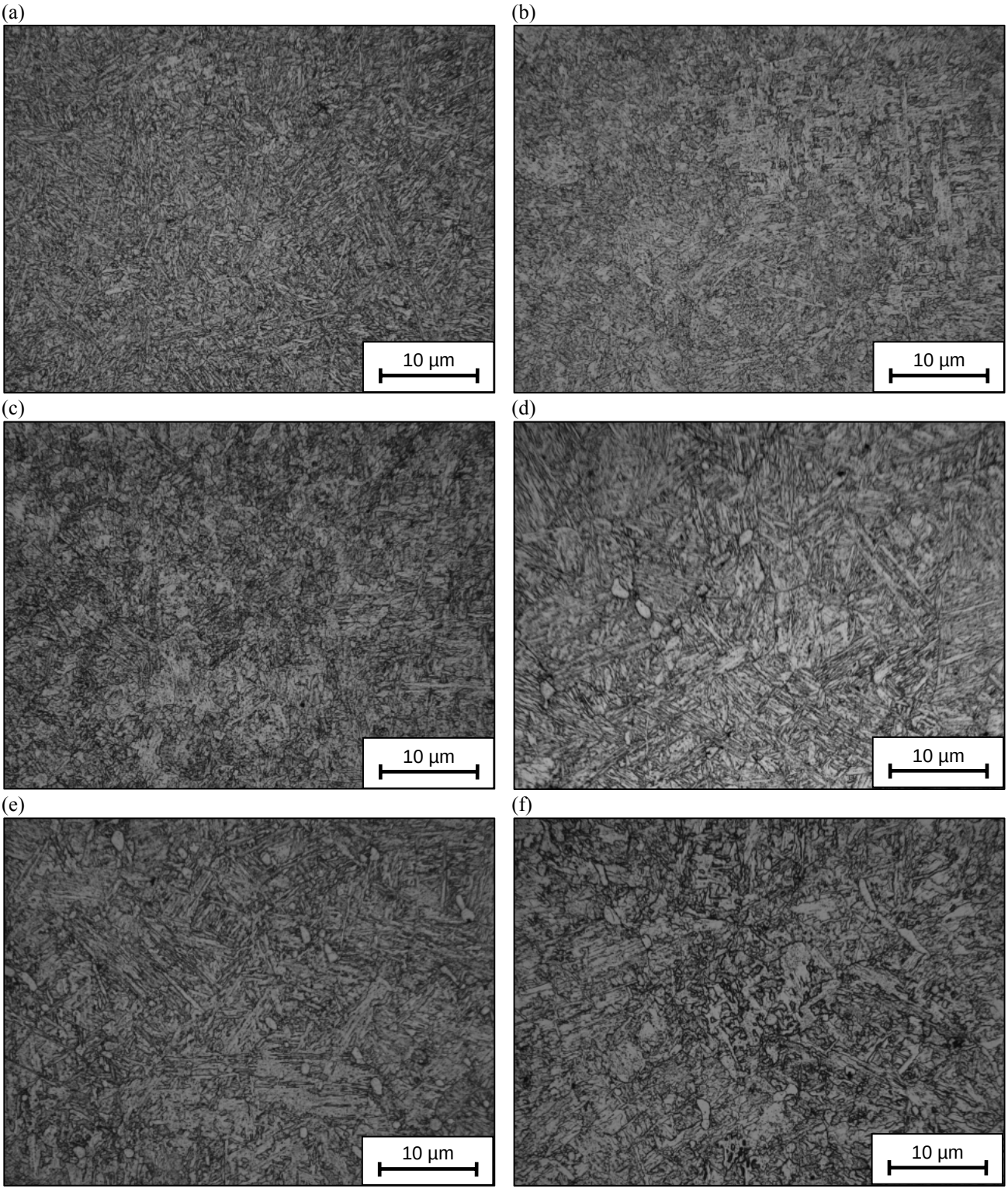

Figure 3: Optical micrographs of the samples after a post weld heat treatment overshoot heat treatment followed immediately by a standard tempering heat treatment at 750^{o}C for 2 hours (a) P91 at 800^{o}C (b) P91 at 860^{o}C (c) P91 at 900^{o}C (d) P92 at 800^{o}C (e) P92 at 860^{o}C and (f) P92 at 900^{o}C.

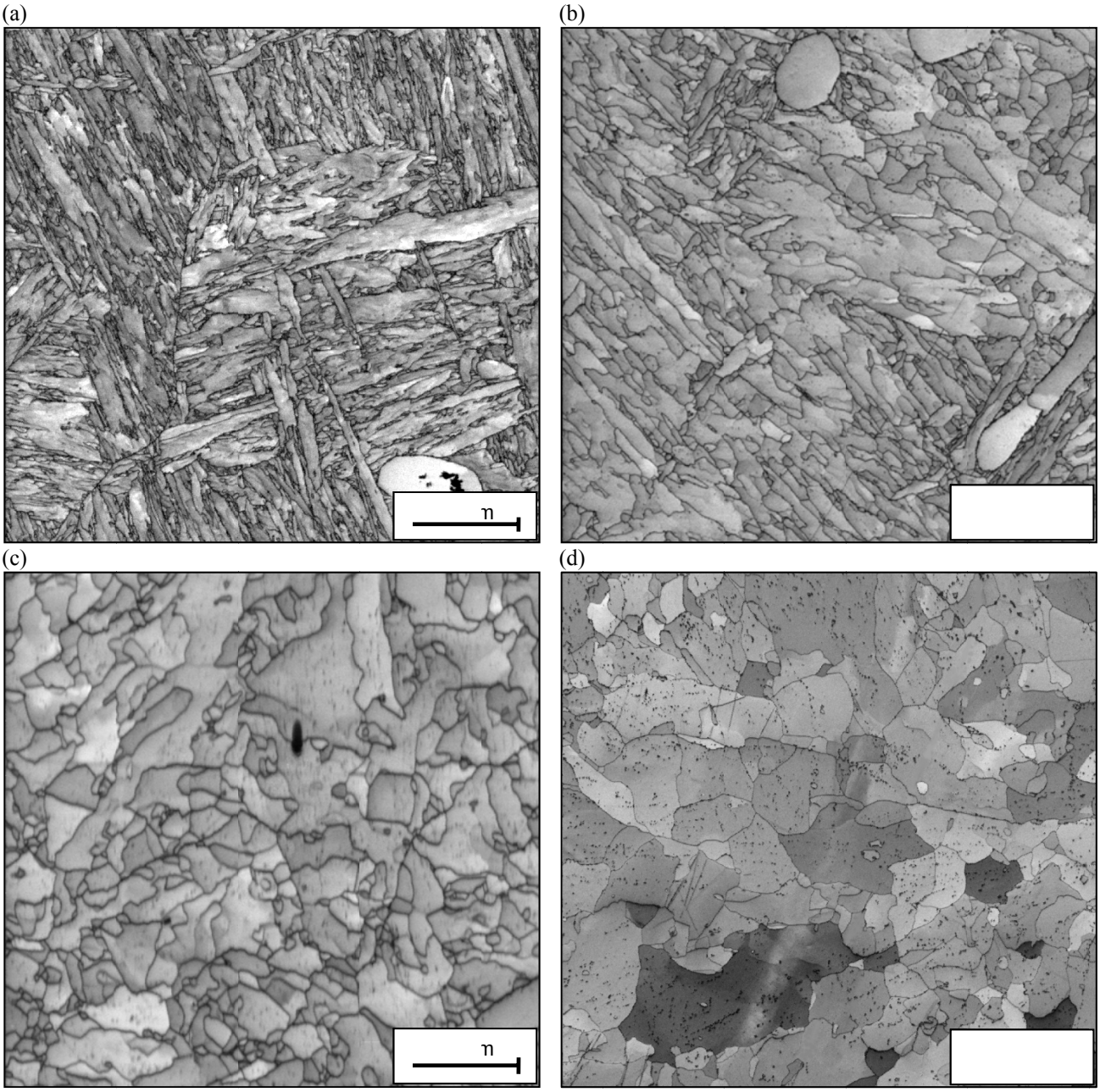

Figure 4: Electron back scatter diffraction image quality maps from the P92 samples given post weld heat treatment overshoot for 1 minute at (a) 800°C (b) 880°C (c) 900 °C and (d) 960°C followed immediately by tempering at 750°C for 2 hours prior to subsequent cooling to room temperature.

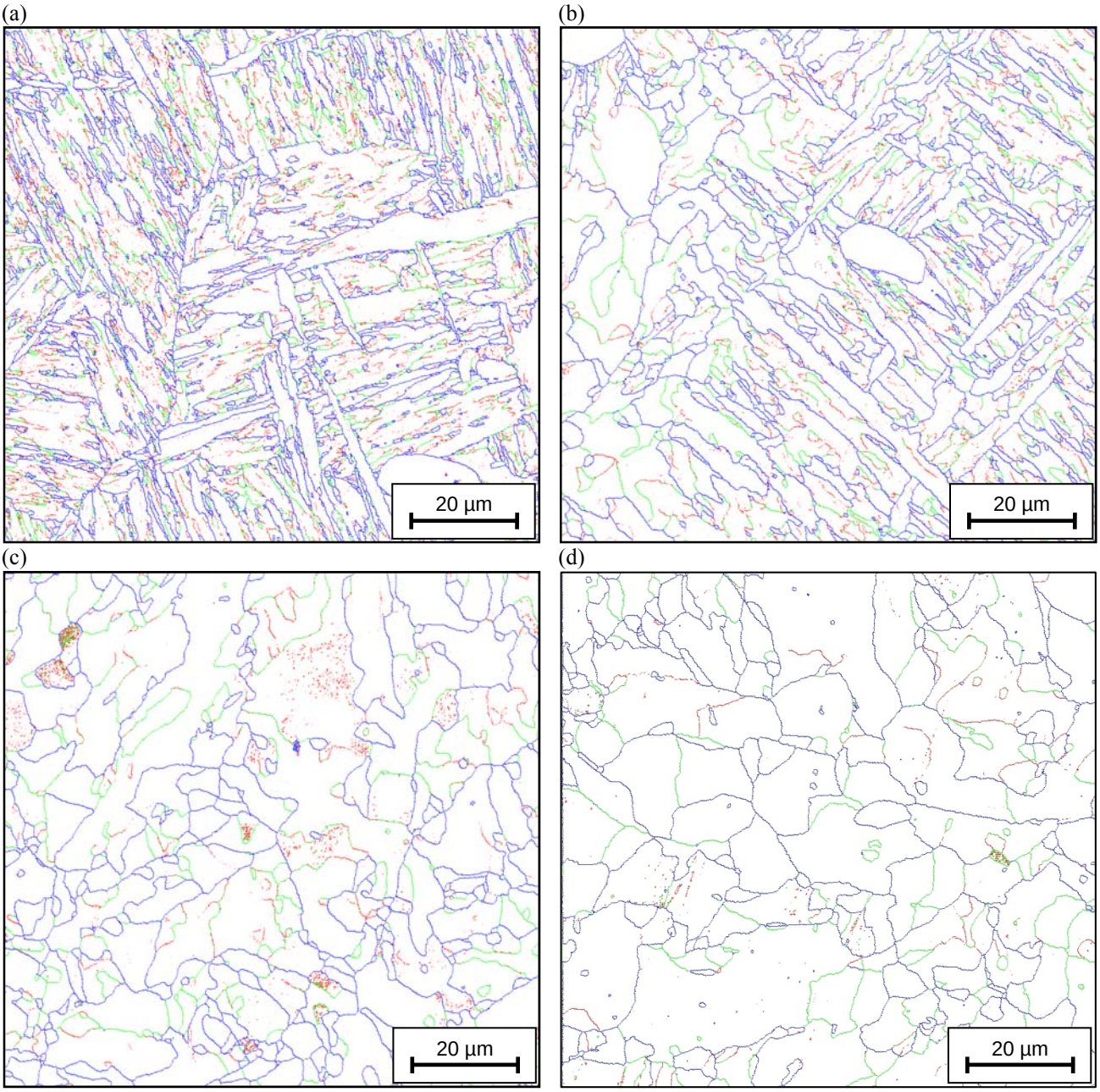

Figure 5: Electron back scatter diffraction grain boundary maps from the P92 samples given post weld heat treatment overshoot for 1 minute at (a) 800°C (b) 880°C (c) 900 °C and (d) 960°C followed immediately by tempering at 750°C for 2 hours prior to subsequent cooling to room temperature. High angle boundaries (blue) represent angles >15°, angles between 5 and 15° are coloured in green, and low angle boundaries are defined to be those <5° and coloured in red.

Use of EBSD allows quantification of the microstructure in respect of the grain boundary length and mean grain size. Whilst automatic determination of the grain size is noted to be subject to error, nevertheless after PWHT to peak temperatures of 800 and 840°C, a consistent grain size was determined of 2.8 µm which is representative of the martensite lath size. At peak temperatures of 860°C and above the grain size determined using EBSD was gradually observed to increase from ~3.5 µm at 860°C, ~6 µm at 900°C to ~10 µm at 960°C. There was also a significant decrease in the length of the high angle grain boundaries observed, from 8 mm at a peak temperature of 800°C to 3 mm at 960°C. These data are consistent with the direct observations from the maps presented in Figure 5, in which it can be clearly seen that there are far fewer high angle grain boundaries at the highest peak temperature.

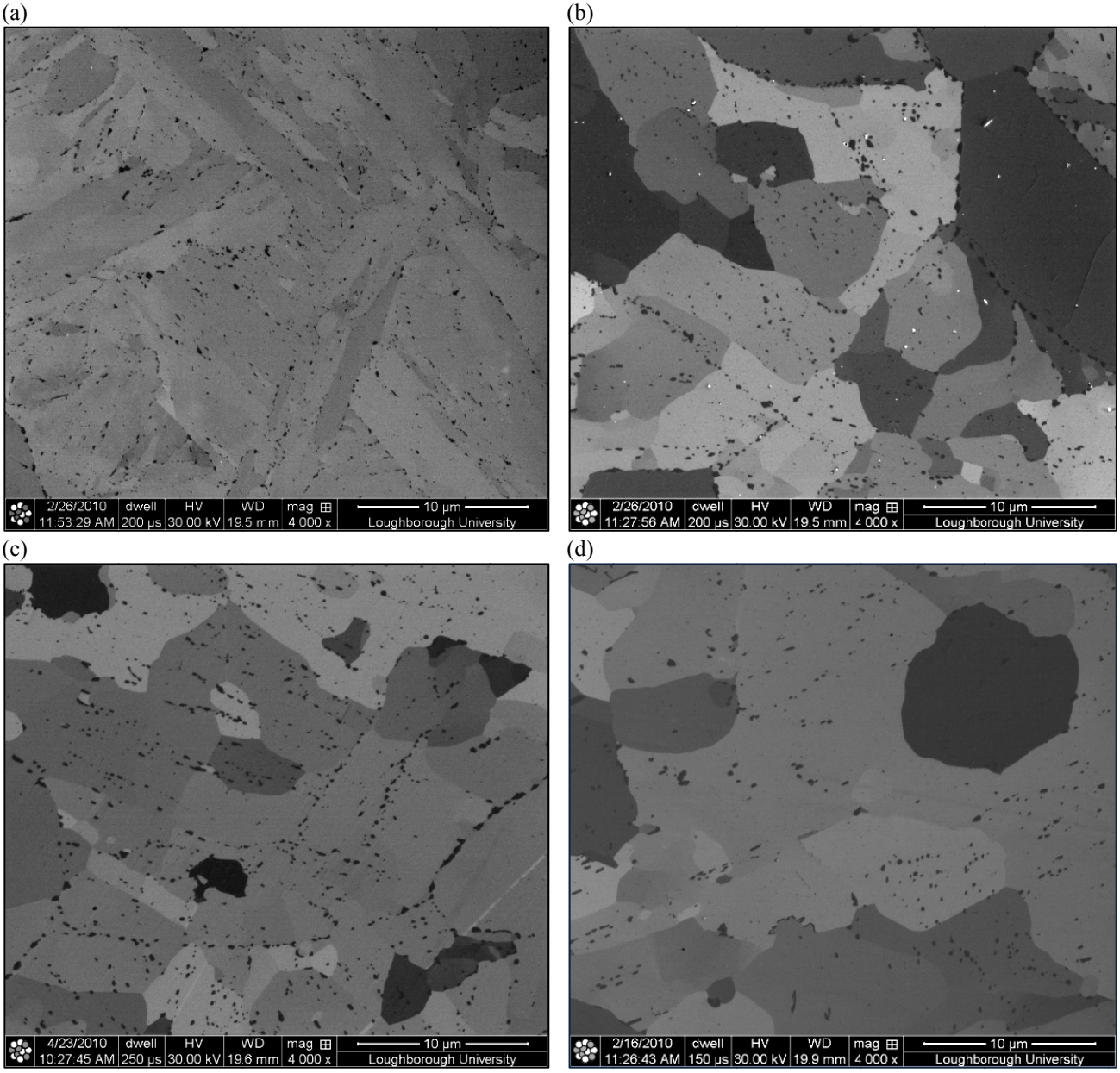

Figure 6: Higher resolution micrographs produced using gallium ion beam imaging in which grain contrast is visible, together also with the large carbides present within the microstructure of the P92 samples given a post weld heat treatment 'overshoot' heat treatment at peak temperatures of (a) 800°C (b) 880°C (c) 900°C and (d) 960°C followed by a standard temper at 750°C for two hours.

Ion beam imaging provides an excellent opportunity to image the nature of the grain structure whilst at the same time being able to observe the larger $M_{23}C_6$ carbides present within the microstructure. Figure 6 presents higher resolution images of the P92 samples given a post weld heat treatment 'overshoot' heat treatment at peak temperatures of (a) 800°C (b) 880°C (c) 900°C and (d) 960°C followed by a standard temper at 750°C for two hours.

Examination of the images shows that initially (Figure 6a) the carbides are exclusively confined to the martensite lath and prior austenite grain boundaries. As the overshoot temperature was increased, the carbide particles can be observed to coarsen significantly, in conjunction with an overall decrease in the number of particles. Image analysis of 5 different ion beam micrographs from each sample indicated a reduction from 1361 particles at a peak temperature of 800°C, to only

420 particles over the same area after a peak temperature of 960°C. It was also noted that the particles remained in lines which appeared to continue to follow prior austenite or martensite lath boundaries, rather than following the grain boundaries present in the microstructure after heat treatment at 750°C in which new, ferritic, grain boundaries appear to have formed. This is particularly evident in Figures 6b and 6c for peak temperatures of 880 and 900°C respectively. Similar behaviour has been previously observed[7] after thermal cycling to 950°C for Grade 92 steel using standard scanning electron microscopy.

Transmission electron microscopy has been carried out on carbon extraction replicas in order to determine the identity and chemical composition of the second phases present within the microstructure as a function of heat treatment. The majority of the carbides observed were found to be rich in Cr, with a mean composition of the metallic elements measured using EDX analysis of ~ 54 wt.% Cr, 25 wt.% Fe, 11 wt.% W, 4 wt.% V and 3 wt.% Mo and small amounts of other elements present in the steel composition. It was noted that there was a slight increase in the concentrations of Nb, Mo and W in the carbides present within the sample which had experienced a peak temperature of 960°C. These data are consistent with the majority carbide being $M_{23}C_6$ as expected, and as predicted by the thermodynamic calculations. A population of smaller particles was also present in all of the samples, which were found to be rich in both V and Nb, with some Cr substitution within the lattice. No Laves phase was observed in the samples, which is consistent with the fact that they had only undergone short term thermal exposure for a maximum of 2 h at 750°C.

3.4 Mechanical Properties

It has been shown above that there is a significant influence on the microstructure as a result of a short excursion to high temperatures above Ac_1 and Ac_3 in particular. Samples which had experienced a peak temperature which was between Ac_1 and Ac_3 (for example, 880°C in this research) contained a 'mixed' microstructure in which there was some evidence of a 'disintegrated' martensitic lath structure, and an indication that more than one matrix phase was present. However, the samples which had undergone the highest peak temperatures above Ac_3, for example 960°C, exhibited a coarse microstructure with large ferrite grains being present and little evidence of the original martensitic structure. Hardness data indicated that these microstructural changes would be accompanied by a significant softening, with drops of ~40-50Hv_{10} compared to the as-received material for both the 'mixed' and the 'ferritic' microstructures.

It is extremely important to determine the influence of such changes in microstructural condition on the mechanical properties of the material in subsequent service conditions, and in particular the likely effect of an excursion to higher temperatures during operations such as post weld heat treatment. Therefore, heat treatments were carried out in furnaces on much larger creep test samples for the P92 material only to recreate the 'mixed' and 'fully ferritic' conditions typical of those observed after the simulated PWHT in the dilatometer at, for example, 880 and 960°C. Microstructural examination after post heat treatment, using the same techniques as described above (hardness, optical, ion beam imaging and EBSD to investigate the resulting grain structures) confirmed that the samples produced for creep testing had the two desired microstructural conditions.

Hardness tests carried out on the 'mixed' and 'fully ferritic' conditions in fact produced very similar values of ~156 Hv_{10} and ~154 Hv_{10} respectively for the two different conditions. These data compare very favourably with the values presented in Figure 2d for the dilatometer heat treatments. In the 'mixed' condition, the ion beam images also indicated that the $M_{23}C_6$ carbides were no longer following grain boundaries in a similar manner to the micrograph shown in Figure 6b.

Creep tests were carried out on the two microstructural conditions at test stresses of 120, 100 and 80 MPa at 625°C in order to obtain data within a reasonable time frame without accelerating microstructural change unduly. It was observed from examination of the failed test pieces that the failures were more ductile in the 'ferritic' condition than in the 'mixed' microstructural condition, with a correspondingly lower number of creep cavities being observed in the 'mixed' condition. The creep data are presented in Figure 7, with failure times for the tests carried out at the two higher stresses of 120 and 100 MPa shown. The lower stress tests at 80 MPa are currently ongoing. The data are compared with the mean failure line for P92 material as determined by the European Creep Collaborative Committee (ECCC)[8] using their formula derived from standard P92 material after typical normalizing and tempering heat treatments. Lines at both 80% and 60% of the parent mean stress line are plotted for comparison purposes. It is clear that the data obtained from the two 'unusual' conditions generated in this research fall well below the mean line, and indeed are more consistent with the line which represents properties which are 60% of that typically expected for P92 material.

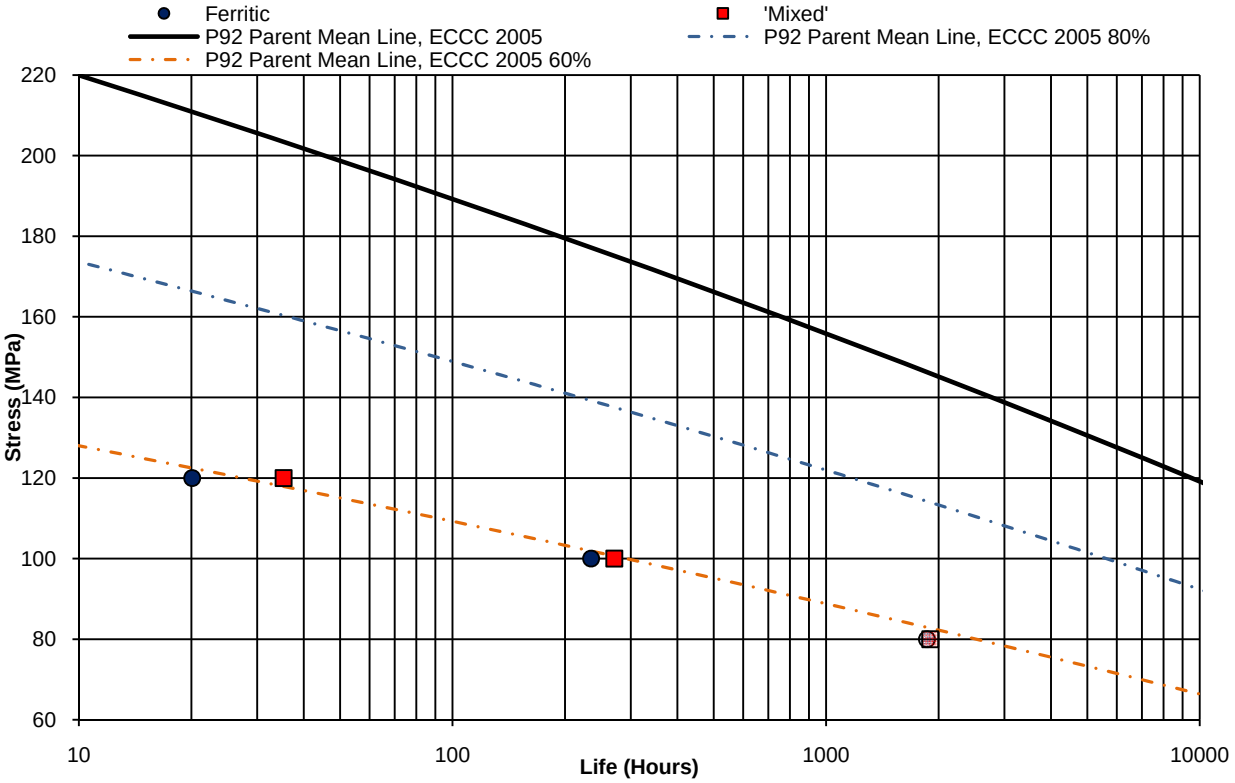

Figure 7: Creep rupture data at 625°C of both the 'mixed' and fully ferritic microstructures compared with mean behavior derived from ECCC 2005 published data.

4. Conclusions

Both P91 and P92 materials have been subjected to brief excursions to high temperatures (above Ac_1 and Ac_3) in order to simulate the effect of an overshoot during a post weld heat treatment cycle. It has been shown that significant changes occur within the microstructure, especially with respect to the matrix microstructure. At overshoot temperatures up to 820°C in P91, and 840°C in P92, there is little change evident to the martensitic matrix and the hardness is maintained. However, as the peak temperature increases above these levels, there is a significant 'disintegration' of the martensitic matrix, leading eventually to the formation of ferrite within the structure during tempering at 750°C and a reduction in hardness of ~50 Hv_{10}. The cycles to increasingly higher temperatures are accompanied by an increase in grain size and a corresponding decrease in the length of the high angle grain boundaries.

There are accompanying changes in the population of the $M_{23}C_6$ carbides. The predicted equilibrium dissolution temperature of $M_{23}C_6$ is ~860^{o}C for P91 and a little higher at ~890^{o}C for P92. During very brief excursions to high temperature, the $M_{23}C_6$ is unable to fully dissolve, but was observed to coarsen significantly. Subsequent holding of the steel at the PWHT tempering temperature of 750^{o}C will result in additional precipitation of $M_{23}C_6$, and indeed MX, leading to a complex precipitate distribution. Importantly, the carbides no longer reside on prior austenite or martensite lath boundaries once a mixed or fully ferritic matrix is produced as a result of the complex heat treatment cycle. The mechanical properties, and particularly creep rupture data, of these mixed and ferritic microstructures are found to be some 60% of the mean value for Grade 92 in a conventionally heat treated condition. The findings of this research have important implications for the service performance of components which may have experienced heat treatments which deviate from the conventional normalizing and tempering conditions.

5. Acknowledgements

We would like to acknowledge the support of RWE NPower for their valuable contribution to this research.

References

[1] K. Haarmann, J.C. Vaillant, W. Bendick and A. Arbab, *The T91/P91 Book*, Vallourec and Mannesmann Tubes (1999).

[2] D. Richardot, J.C. Vaillant, A. Arbab and W. Bendick, *The T92/P92 Book*, Vallourec and Mannesmann Tubes (2000).

[3] J. Orr and D. Burton, *Ironmaking and Steelmaking*, **20**, p. 335, 1993.

[4] R.H. Davies, A.T. Dinsdale, T.G. Chart, T.I. Barry and M.H. Rand: *High Temperature Science*, **26**, p 251, 1989.

[5] B. Sundman: TCFE database supplied by TCAB for use with MTDATA, 2000.

[6] G. West and R.C. Thomson, *Proceedings of Parsons 2007 Power Generation in an Era of Climate Change*, Eds. Strang, A., Banks, W.M., McColvin, G.M., Oakey, J.E., Vanstone, R.W., IOM Communications Ltd, Glasgow, UK, September 2007, p 521, 2007.

[7] F. Abe, M. Tabuchi, S. Tsukamoto and T. Shirane, *Proceedings of Welds 2009*: Design, Testing, Assessment and Safety of High Temperature Welded Structures, June 2009, Fort Myers, Florida, USA, 2009.

[8] European Creep Collaborative Committee (ECCC) Datasheet on Steel ASTM Grade 92 (BS PD6605), 2005.